Corrosion Behavior of ESR Produced Nickel Free High Nitrogen Austenitic Stainless Steel

P. Saravanan*, V. S. Raja

Department of Metallurgical Engineering and Materials Science, Indian Institute of Technology Bombay, Powai, Mumbai, India

Abstract

Corrosion behavior of 19Cr-18Mn-0.69N austenitic stainless steel (SS) developed by electroslag refining process (ESR) was studied by cyclic polarization technique in 3.5% NaCl solution and was compared with that of the other two austenitic stainless steels having different compositions namely, Type 316L SS and 14Cr-8-Mn SS. The results showed that 19Cr-18Mn-0.69N austenitic stainless steel far exhibits higher pitting potential as compared to that of the other two alloys. The ESR melted alloy also better crevice resistance than that of Type 316L SS and 14Cr-8-Mn SS alloy. However, the degree of improvement in the crevice corrosion resistance of ESR melted alloy over the remaining two alloys is lower than that obtained with regards to pitting corrosion resistance. The high pitting and crevice corrosion resistance of ESR melted alloy, in spite of its higher sulfur content than similar alloys published in literature, is attributed to the ability of ESR technique to minimize the sulfur inclusions in stainless steels.

1. Introduction

Nickel containing austenitic stainless steels (SS), such as Types 304 and 316 SS has been workhorse for a variety of industrial applications. The rise in the cost of nickel has been a problem for stainless manufactures in containing the cost of stainless steels [1-6]. Moreover for body implants nickel in SS is unwanted as it is found to be toxic to the human body [7 and 8]. These factors enabled development of nickel free austenitic stainless steels with manganese as a substitute element. Manganese stabilizes the austenitic phase, like nickel, and costs much lesser than nickel are the reasons for its use in place of nickel. There has been some work on the corrosion studies of manganese substituted stainless steels [9-15]. Some of these studies indicate that manganese is beneficial to pitting and crevice corrosion [9], while a few of them [10 and 11] show that manganese is detrimental to the pitting resistance of stainless steels, but few say it is detrimental above certain level [12 and 13]. Examination of the studies reported in the literature suggests that manganese can be less detrimental if the environment is less aggressive. Thus, Lunsarska et al., [14] have reported a significant drop in pitting potential (E_{pit}) of 18Cr-5Ni SS in 0.1N H_2SO_4+0.1N NaCl, due to manganese addition. But the Mn containing alloy exhibited the same E_{pit} as that of manganese free alloy when the chloride level in the sulfuric acid is reduced to 0.1N H_2SO_4+0.01N NaCl

One of the beneficial effects of manganese is that it enables high nitrogen addition to stainless steels. Nitrogen being an efficient element to promote pitting resistance of stainless steels, the presence of nitrogen in Mn containing stainless steels is expected to enhance their pitting resistance. Recent study by Lim et al., [15] shows that Mn is detrimental to pitting corrosion even if it has high nitrogen content. They have found that even 0.17 wt% N in Type 316L SS can give rise to an E_{pit} of about 1200 mV (vs SCE) in 1M KCl, while

* Corresponding author

E-mail address: sarvan@sail-rdcis.com (P. Saravanan)

Type 316L SS added with 20 wt% Mn and 0.394 wt% N exhibits E_{pit} below 400 mV (vs SCE), (a value less than that 450 mV (vs SCE)) exhibited even by N free Type 316L SS) in spite of this alloy having high nitrogen level. Examination of passive current densities of manganese free and manganese containing Type 316L SS however, showed both of them to have almost similar values, though they differ in E_{pit} values. These authors have implicated the low pitting resistance of the alloy to the presence of MnS inclusions in Mn containing stainless steel. It will be therefore interesting to examine high manganese stainless steels with less MnS inclusions. This study concerns with examining the passivity and pitting and crevice corrosion tendency of 18Cr-18Mn SS (Table I) produced through eletroslag refining process (ESR). This process has the ability to refine the alloy to lower its inclusion content [16 and 17].

Another interesting point is that most of the manganese stainless steels are developed with Mo and N. Addition of Mo adds up to the cost of stainless steel. To our knowledge, literature on Mo free high nitrogen high manganese alloys is scanty only one author [18] has worked on the corrosion behavior of Mo free high manganese high nitrogen stainless steels. They reported that high Mn high N SS (Mo free) show very low pitting resistance compared to Type 316L SS. In India one such steel (18Cr-18Mn nickel free high nitrogen austenitic stainless steel) has been produced by Electro-slag Refining process (ESR).This alloy is found to have a good combination of strength and toughness [19], but its corrosion

behavior is unknown. Hence the present study is focused on the detailed examination of corrosion behavior for ESR melted Mo free high Mn and high N stainless steel. Two more alloys namely Type 316L SS and a moderate level Mn containing alloy (14Cr-8Mn SS) (Table I) are also examined for comparison. The medium level manganese is produced by argon-oxygen decarburization (AOD) process.

2. Experimental Method

2.1. Materials and Microstructures

The alloy 19Cr-18Mn-0.69N SS melted by ESR technique was cold rolled and the solution was treated at 1150°C for 1h.The other two alloys namely, Type 316L SS and 14Cr-8Mn SS are commercially available were solution treated at 1050°C for 1h. The chemical compositions of the alloys examined in the study are shown in Table I.

To examine the resistance of the alloy to intergranular attack (IGC), specimens were electrolytically etched as per ASTM A 262 A [20] in a solution of 10% oxalic acid at room temperature. Samples were etched for 90 s at a current of $1A/cm^2$ by keeping them as an anode and a platinum sheet as a cathode. After etching, the microstructures of the specimens were observed in an optical microscope. As the samples exhibited step-structure, indicative of the alloys intergranular corrosion resistance, they were used for further studies.

Table I. Chemical composition of the austenitic stainless steels (wt%).

Alloys	C	Mn	S	P	Si	Ni	N	Cr	Mo
19Cr-18Mn-0.69N SS	0.070	18.07	0.011	0.043	0.37	----	0.69	19.59	---
14Cr-8Mn SS	0.063	8.22	0.018	0.070	0.27	2.74	----	14.79	---
Type 316L SS	0.025	1.52	0.010	0.026	0.49	11.6	----	17.81	2.65

2.2. Polarization Tests

Electrochemical polarization behavior of the alloys was studied using a set-up that consisted of PARC, EG & G potentiostat/galvanostat (Model 273 driven by M352 software) and an electrochemical corrosion cell.The corrosion cell was a glass vessel, as specified in ASTM G5-94 [21], with 1000 ml capacity.The cell consisted of a platinum sheet as a counter electrode, saturated calomel electrode (SCE) as a reference electrode and specimen as a working electrode. Freely exposed 3.5% NaCl solution was chosen as an electrolyte. The sample specimens were hot mounted leaving one face of the sample with $1cm^2$ area freely exposed, and electrical connection was provided by drilling backside of the mount and soldering the copper wire to the sample, finally sealing the hole by cold cure resin. The samples were ground till 4/0 grade silicon carbide paper and finally wet polished using alumina powder. To avoid crevice

corrosion of the sample, mount-sample interface was carefully coated with a thin araldite sealant.

Cyclic polarization experiment was carried out to study the passivation and repassivationbehaviors of the alloy.The potential was scanned from -300mV with respect to open circuit potential (OCP) with a scan rate of 0.5mV/s to a potential at which the current density reached $5mA/cm^2$ and then the scan was reversed to reach OCP.

2.3. Ferric Chloride Test

The ferric chloride solution test based on the practice MTI-2 (Materials technology institute of the chemical process industry) [22] modified practice of ASTM G48 standard [23] was conducted. For this, specimens of 50x25x3 mm dimension with a surface finish of about 600 grit were used. Multiple crevice assembly device used in the study consisted of two serrated teflon (PTFE) washers. Each of these washers provided 12 grooves. When fastened on to a plate specimen

to form a crevice assembly, these grooves produced a total of 24 crevice sites on both the sides of the specimen. The washers, one on each side, were initially secured at a specified torque of 0.28Nm. The whole crevice assembly was immersed in 800ml of 6% ferric chloride ($FeCl_3 \cdot 6H_2O$) solution for 24h duration. The starting test temperature of the solution was calculated based on the following equation that relates the crevice corrosion temperature (CCT) to the alloy composition [23].

$$CCT = 3.2\%Cr + 7.6\% Mo + 10.5\% N - 81 \quad (1)$$

Subsequent tests were conducted either by lowering or rising the test solution temperatures in steps of 5°C. Tests were continued to find the highest temperature at which specimens suffered an attack just lower than 25μm, This is because, as per the ASTM standard an attack exceeding 25μm deep on a specimen qualifies to be called as a crevice attack. The number of crevice sites observed on each of the alloy above CCT is also reported.

3. Results and Discussion

3.1. Polarization Test

Cyclic polarization curves of all the three alloys are compared in Fig. 1. The electrochemical kinetic parameters namely, corrosion potential (E_{corr}), passive current density (i_{pass}), and pitting potential (E_{pit}) for these alloys were obtained from the curves and summarized in Table II. As there is no potential independent current region (typical of an ideal passive system) in the anodic polarization curve, the passive current density exhibited by the alloys at 100mV (vs SCE) has been compared. Following observations can be made on the basis of the data summarized in Table II. 19Cr-18Mn-0.69N SS shows a lower passive current density (i_{pass}) by an order of magnitude, compared to that of 14Cr-8Mn SS. But the former exhibits a relatively higher i_{pass} than that of Type 316L SS. Notably, 19Cr-18Mn-0.69N SS shows a significantly higher E_{pit} as compared to both the other alloys. Thus, E_{pit} of 19Cr-18Mn-0.69N SS, Type 316L and 14Cr-8Mn SS were found to be 1050, 280, and -80mV (vs SCE) respectively. The possible role of manganese and nitrogen on the pitting tendency of the alloy is discussed below.

The work by Lim et al., [15] on the investigation of the role of manganese and nitrogen on pitting corrosion behavior of Type 316L SS is interesting. They showed that the alloy 20.2Mn-14Ni-18Cr-0.394N, obtained through manganese and nitrogen addition to Type 316L SS, exhibited lower E_{pit} than Type 316L SS in 1M KCl solution even when the former had 0.394 wt% N. On the contrary the present high manganese stainless steel exhibited far higher E_{pit} value than that of Type 316L SS. The occurrence of lacy type of pits is responsible for low E_{pit} values of 20.2Mn-14Ni-18Cr SS-0.394N, where as the present high manganese stainless steel did not show any pits (Fig. 2) even after subjecting it to about 1.5V (vs SCE). Interestingly, the medium level Mn stainless steel (14Cr-8Mn SS) not having N shows large amount of lacy type of pits, despite the fact that it is subjected a much lower anodic potential than 19Cr-18Mn-0.69N SS. Notably, Type 316L does not show such type of pits. Generally, sulfur is considered to be detrimental to pitting resistance. In the present study, the role of sulfur on pitting is less apparent. Comparison of sulfur levels of all three alloys under study indicates that sulfur levels are almost the same (0.01-0.018 wt %), even though the alloys show different pitting tendency. For example, Type 316L SS and 14Cr-8Mn SS have similar sulfur levels but exhibit different types of pit morphology. It is known that manganese promotes MnS inclusions. Thus the difference in pitting behavior of these two stainless steels can be attributed to high manganese content of 14Cr-8Mn SS than Type 316L SS and consequent high MnS inclusions present in the former than the latter. However, the ESR produced 19Cr-18Mn-0.69N SS has the same sulfur level as that of the two alloys and higher manganese content than 14Cr-8Mn SS, yet shows higher E_{pit} than the other two alloys. Thus manganese percentage can not be attributed to the poor pitting resistance of 14Cr-8Mn SS. Regarding the role of sulfur on the pitting resistance of the manganese containing SS, it is instructive to look at the sulfur levels of 20.2Mn-14Ni-18Cr-0.394N alloy (produced by vacuum induction melting) that was studied by Lim et al.,[15]. This alloy exhibited lower E_{pit} of 400mV (vs SCE) than the present alloy (19Cr-18Mn-0.69N SS) even though it had 0.001 wt% S. Thus pitting resistance of the alloy cannot be related to mere S content of the alloy, as it depends on the ability of sulfur in the alloy to form MnS inclusions. ESR process lowers the inclusions in stainless steels. The progressive solidification of the melt, as the electrode gradually melts, makes the sulfur to uniformly distribute in the cast and discourages inclusion formation [15 and 17]. Hence, the absence of sulfide inclusions in ESR melted alloy makes 19Cr-18Mn-0.69N SS more resistance to pitting than 14Cr-8Mn SS and Type 316L SS.

The above proposition lends credence from the following facts. Mohamed et al., [18] showed that the SS 15Cr-14Mn-0.28N (produced by induction melting) possessed a pitting potential of -20mV (vs SCE) in 1N NaCl solution, which is significantly lower than the pitting potential of the present ESR produced alloy, namely, 19Cr-18Mn-0.69N SS. Though the current alloy has a marginally higher level of chromium and nitrogen levels, than the alloy studied by Mohamed et al., [18] the vast difference in E_{pit} between the two alloys (from −20mV to 1050mV (vs SCE)) can not be attributed the mere

compositional variation. The pitting resistance between the alloys can therefore be attributed to the differences in the production processes that affect sulfide inclusion formation. The literature also indicates that when high manganese and high nitrogen is produced through a process that eliminates

sulfide inclusion formation, then the alloy can posses high pitting resistance. Thus 17Cr-12Mn-3Mo-0.9N SS produced by powder metallurgy route exhibited high E_{pit} value of 1200 mV (vs SCE) in artificial seawater [24].
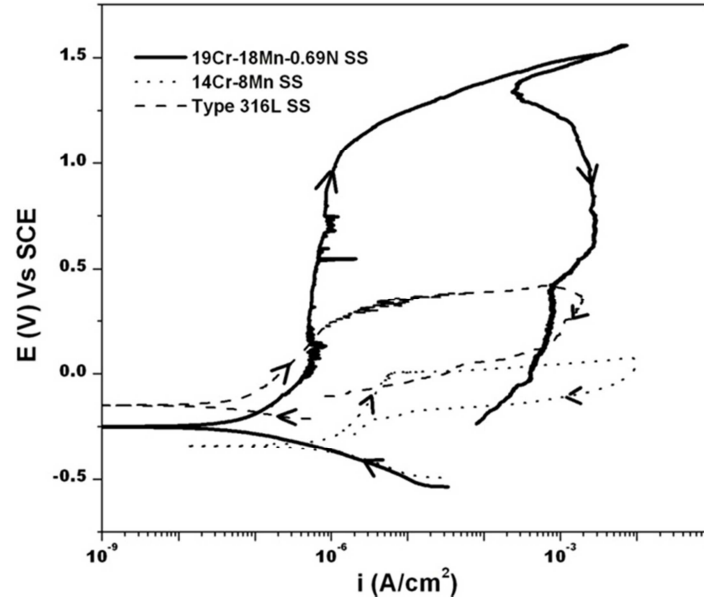

Figure 1. Cyclic polarization curves of three austenitic stainless steels obtained in 3.5% NaCl.
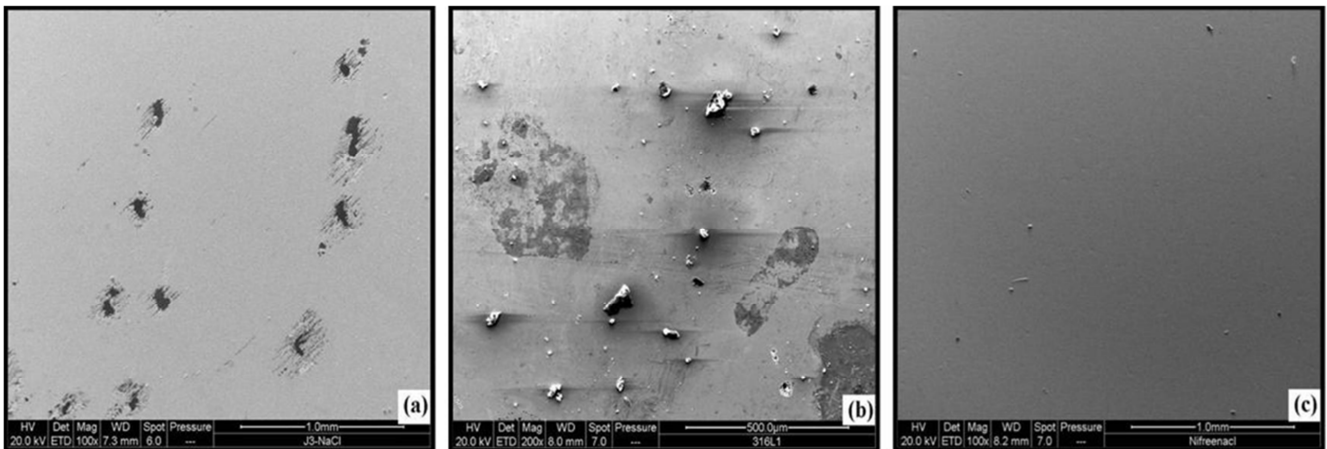

Figure 2. Secondary Electron Microscopic image of (a) 19Cr-18Mn-0.69N SS (b) 14Cr-8Mn SS and (c) Type 316L SS observed after the polarization test.
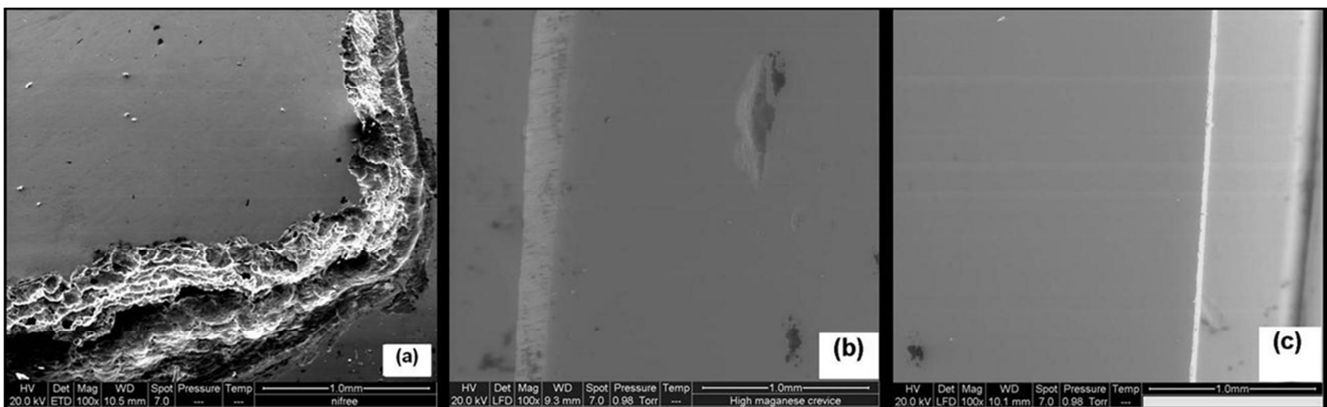

Figure 3. Secondary Electron Microscopic image of the interface of (a) 19Cr-18Mn- 0.69N SS (b) 14Cr-8Mn SS and (c) Type 316L SS after polarization test.

Table II. Electrochemical parameters of the alloys derived from the polarization curves obtained in 3.5% NaCl.

Alloys	i_{pass}, A/cm^2 at 100mV (vs SCE)	E_{pit} in mV (SCE)
19Cr-18Mn-0.69N SS	4×10^{-7}	1050
14Cr-8Mn SS	8×10^{-6}	-80
Type 316L SS	2×10^{-7}	280

The alloy was found to be free from any pits when observed after the polarization test, even in 22% NaCl solution. As a consequence the protection potential (E_{prot}) of the alloy was found to be the same as that of its E_{pit}. Notably molybdenum and nitrogen exert a far greater influence in powder metallurgy produced high manganese SS while the same did not happen in 20.2Mn-14Ni-18Cr-0.394N alloy produced through vacuum induction melting because of the formation of sulfide inclusion [16].

Examination of polarization curves of these alloys show positive hysteresis. But, what is interesting is that 19Cr-18Mn-0.69N SS exhibits the largest hysteresis loop among the three alloys in spite of the fact that this alloy exhibits a far higher E_{pit} than the remaining alloys. Further, Type 316L SS and 14Cr-8Mn alloys posses E_{prot} close to that of their E_{corr}. On the other hand 19Cr-18Mn-0.69N alloy has its E_{prot} below E_{corr}, although this alloy did not suffer pitting during the polarization test (Fig. 2). As this alloy was subjected far higher anodic potential than the other two alloys such an effect may be due to the crevice corrosion attack on the alloy. Hence edges of the alloys are examined. From Fig. 3, it is obvious that 19Cr-18Mn-0.69N SS specimen indeed suffered severe attack at the interface (araldite/metal interface), where

as no such attack was seen on Type 316L and less attack is seen on 14Cr-8-Mn SS specimens. While the above data suggests high susceptibility of 19Cr-18Mn-0.69N SS to crevice corrosion, it should be noted that this alloy was subjected to a far higher anodic potential than rest of other two alloys. This could be the one of the reasons, why the alloy suffered severe crevice corrosion.

Attempts to eliminate crevice attack on the alloy/mount interface were not fully successful. Hence the following types of the experiments were carried out to examine this aspect and to find true susceptibility of the alloy to crevice corrosion.

3.2. Reversal at Different Potentials

19Cr-18Mn-0.69N SS was subjected to cyclic polarization with lower apex potentials than E_{pit} reported earlier. Cyclic polarization curves obtained for a few scans reversed at 300, 600 and 800mV (vs SCE) apex potentials are shown in Fig. 4. As seen, all the reverse scans exhibit lower passive current density than that of the forward scan. Even though all these cyclic polarization curves obtained up to 800 mV (vs SCE) as apex potential show a negative hysteresis loop, indicating stable passivity, microscope examination (Fig. 5) of the polarized specimen reveals crevice attack on those samples scanned with apex potential of 600mV (vs SCE) and above. The apex potential below which the alloy was found to be resistant to crevice corrosion (500 mV (vs SCE)) happens to be higher than E_{pit} values of the other two alloys. Thus the alloy seems to have reasonable ability to resist crevice corrosion.
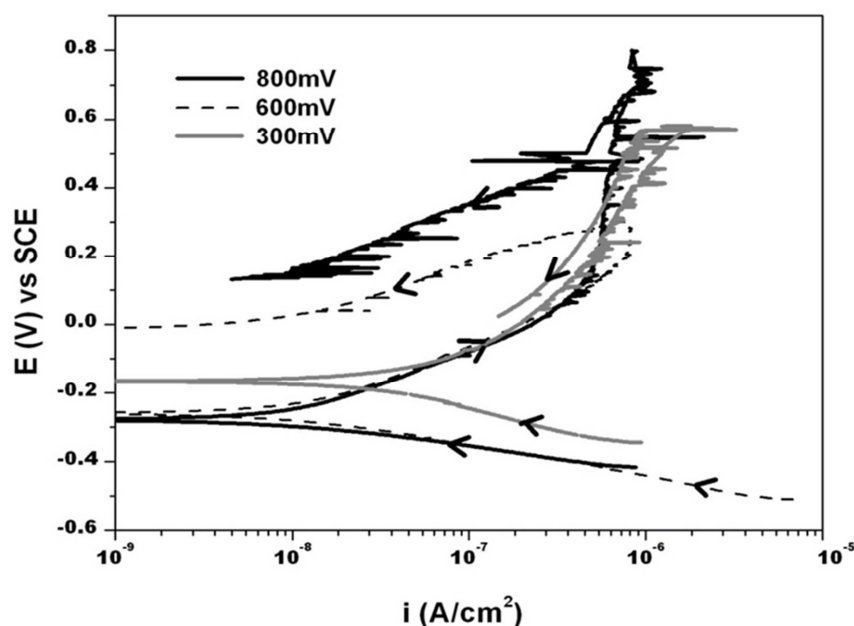
Figure 4. Cyclic polarization curve of 18Cr-18Mn-0.69N stainless steel in 3.5%NaCl for different potential of reversal.
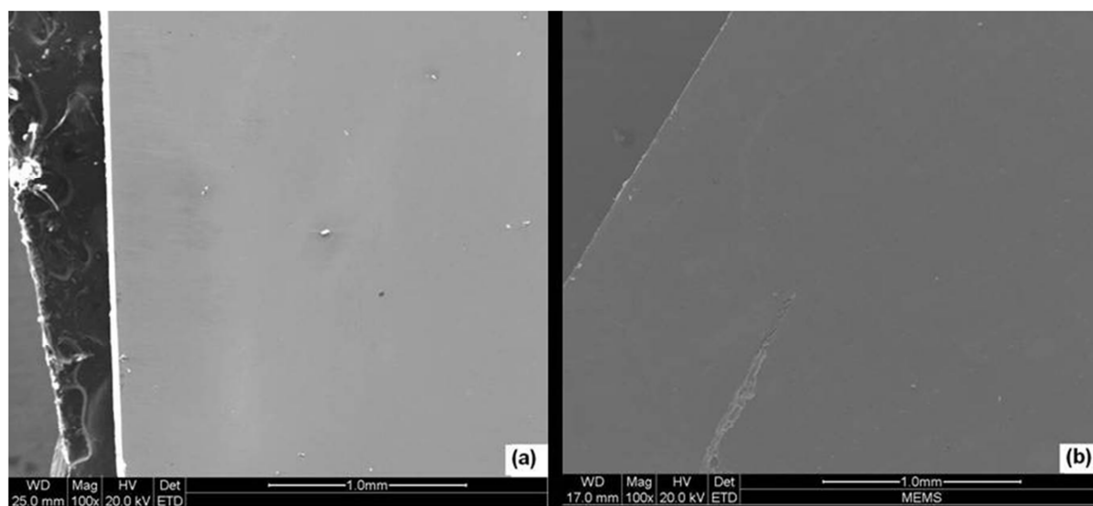
Figure 5. Secondary Electron Microscopic image of 19Cr-18Mn-0.69N after reversalat a) 400 mV (Vs SCE) b) 600mV (Vs SCE).
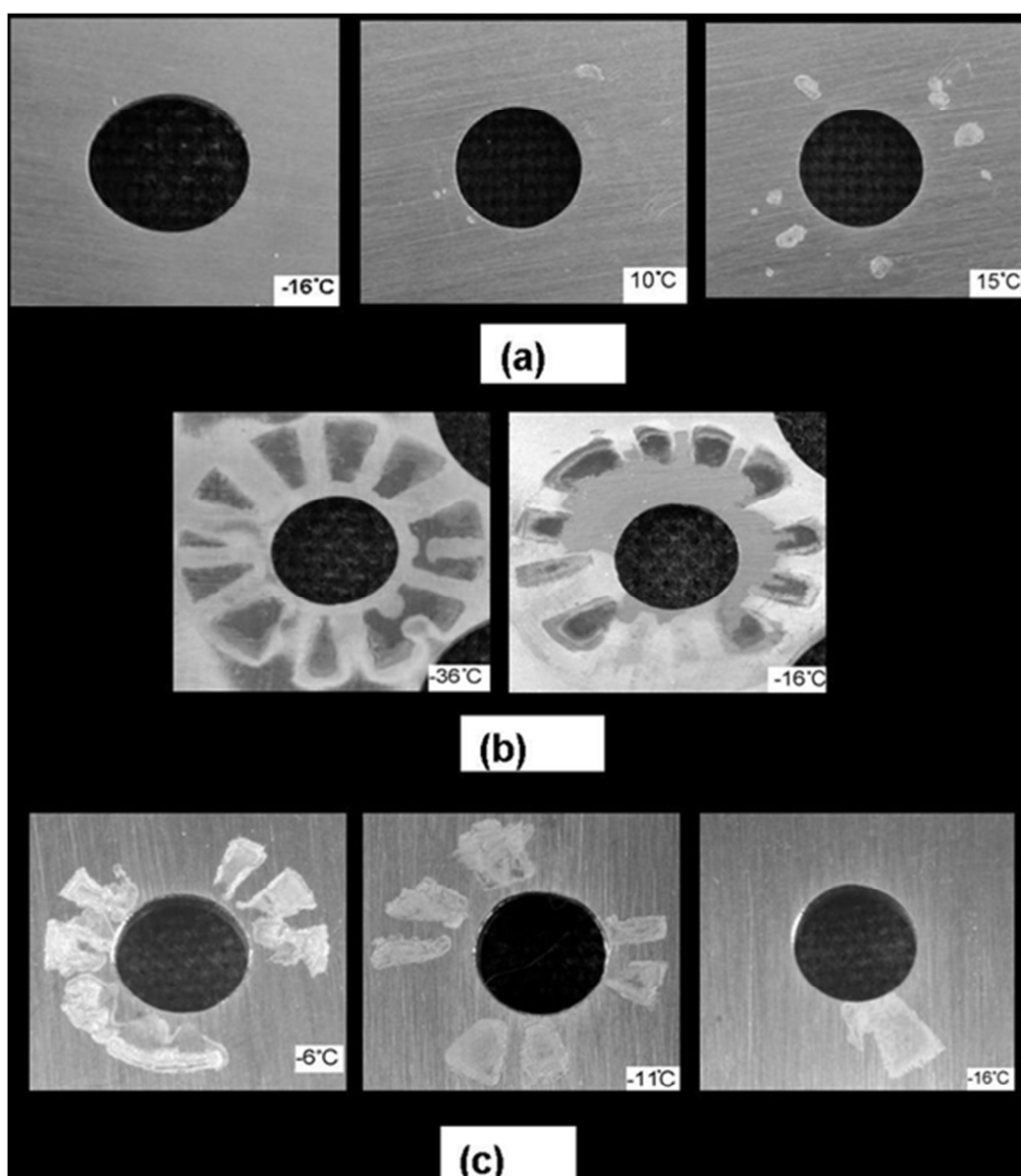
Figure 6. Crevice attacks of (a) 19Cr-18Mn-0.69N SS (b) 14Cr-8Mn SS and (c) Type316L SS in 10% Ferric chloride solution after 24h of immersion.

3.3. Crevice Corrosion Test

In order to evaluate the crevice corrosion resistance of 19Cr-18Mn-0.69N SS, the alloy was subjected to crevice corrosion test as per MTI-2 [22] (modified ASTM standard G48).The starting crevice temperature calculated as per the equation (1) and was found to be -6°C for Type 316L SS, -32°C for 14Cr-8Mn SS and -8°C for 19Cr-18Mn-0.69N SS. The above equation doesn't seem to applicable to the present condition and hence tests were conducted over a wide temperature range than given by the equation (1). A few typical photographs of the samples subjected to crevice test are shown in Fig. 6 and the depth of attack is summarized in Table III. The CCT for Type 316L SS, corresponding to 5μm deep attack, was found to be -16°C. At-16°C the depth of attack for all the alloys are compared (Table III) to evaluate

the relative performance of Type 316L SS with the other two alloys. At this temperature 14Cr-8Mn SS suffered crevice attack of 50 μm at 9 sites while Type 316L SS suffered 5μm a crevice attack and no attack was found over19Cr-18Mn-0.69N SS (Fig. 6). The CCT for 19Cr-18Mn-0.69N SS was found to be 10°C and 14Cr-8Mn SS of about -36°C. Hence from this study it can be said that 19Cr-18Mn-0.69N SS has higher crevice corrosion resistance than that of other two alloys. This supports the cyclic polarization results presented earlier [24]. It is instructive to mention the fact that 17Cr-12Mn-3Mo-0.9N SS, produced through powder metallurgy route, exhibits even higher CCT values (25-35°C) than the present ESR produced alloy (10°C). Accordingly, it can be said that molybdenum and nitrogen in high manganese SS will be very effective if the formation of sulfide inclusions is prevented and ESR technique enables this.

Table III. Depth of crevice attack (*given for comparison).

Materials	Crevice critical temperature	Depth of attack in μm	Number of sites of attack (Depth >25μm)
	-16^0 C*	No attack	0
	-8^0 C	No attack	0
19Cr-18Mn-0.69N SS	5^0 C	4	0
	10^0 C	15	0
	15^0 C	>50	3
	-36^0C	15	0
14Cr-8Mn SS	-31^0 C	>50	6
	-16^0 C*	>50	9
	-16^0 C	5	0
Type 316L SS	-11^0 C	>50	6
	-6^0 C	>50	8

4. Summary

Development of nickel free austenitic stainless steels for corrosion resistant applications is an important subject of study by several investigators. Manganese is found to be an ideal element to replace nickel in austenitic stainless steels. Though manganese is a less noble element than nickel, the ability of the former to increase the nitrogen level of the austenitic stainless steels is considered to be a beneficial factor towards enhancing the localized corrosion resistance of the stainless steels and to offset the corrosion resistance loss due to nickel replacement. This paper brings out the fact that the presence of molybdenum and nitrogen in high manganese stainless steels [15, 19] is less effective in promoting the localized corrosion resistance. The present study further concludes that sulfide inclusions are detrimental in harnessing the beneficial effects of molybdenum and nitrogen. To realize the beneficial effect of molybdenum and nitrogen, formation of these inclusions should be minimized. Such a change is brought out in ESR melted 19Cr-18Mn-0.69N SS and so it could exhibit very high pitting resistance. The work of Uggowitzer et al [24] shows that even powder

metallurgy route of producing inclusion free high manganese alloy (17Cr-12Mn-3Mo-0.9N SS), with high levels of nitrogen and small amount of molybdenum, can exhibit high pitting and crevice resistance. However, ESR technique is for more economical than powder metallurgy technique. Accordingly it is suggested ESR produced 19Cr-18Mn-0.69N SS be further alloyed with molybdenum to further enhance its crevice corrosion resistance.

Acknowledgement

References

[1]   D.J. MILLS and R.D. KNUTSEN, *Wear*1998, 215,83.

[2]   A.H. BOTT, F.B. PICKERING and G.J. BUTTERWORTH, *J. Nucl. Mater.* 1986, 141-143, 1088.

[3]   F.A. GARNER, H.R BRAGER, D.S. GELLES and J.M. Mc CARTHY, *J. Nucl. Mater.* 1987, 148, 294.

[4]   Y. HOSOI, Y. OKAZAKI, N. WADE and K. MIYAHARA, *J. Nucl. Mater*. 1989, 169,257.

[5]   K.H. Lo, C.H. Shek , and J.K.L. Lai, Materials Science and Engineering R, 2009, 65, 39.

[6]   Z. Yuan, Q. Dai, X. Cheng, K. Chen, W. Xu, *Materials Science and Engineering A* 2008, 475, 202.

[7]   D. KURODA, S. HIROMOTO, T. HANAWA and Y. KATADA, *Mater. Trans*. 2002, 43, 3100.

[8]   A. DISCHINO, J.M. KENNY and M. BARTERI, *J. Mater. Sci. Lett*. 2003, 22, 691.

[9]   R.J. BRIGHAM, E.W. TOZER, *Corrosion*, 1976, 32 (7) 274.

[10] R. BANDY, D. VAN ROOYEN, *Corrosion*, 1983, 39 (6) 227.

[11] H. BABA, T. KODAMA and Y. KATADA, *Corros. Sci.* 2002, 44, 2393.

[12] A. CONDYLIS, F. BAYON, and A. DESESTRET, *Rev. Metallurgie.* 1970, 67 (5) 427.

[13] El DIN. A.M SHAMS, M.M. BADRAN and S.E. KHALIL, *Werkst. und. Korrosion*. 1972, 23,576; and *Werkst. und. Korrosion*, 1973, 24, 23.

[14] E. LUNARSKA, Z. SZKLARSKA-SMIALOWSKA and M. JANIK-CZACHOR, *Corrosion* 1975, 31 (7) 231.

[15] Y.S. LIM, J.S. KIM, S.J. AHN, H.S KWON, and Y. KATADA, *Corros. Sci.* 2001, 43, 53.

[16] G. HOYLE, in "Electroslag Processes—Principles and Practice" (Applied Sci. Pub. London, 1983), p. 50, 56, 75.

[17] G. BALACHANDRAN, "Studies on processing & structure property correlation in 18-Cr-18Mn nickel free high nitrogen austenitic stainless steel" PhD Thesis *IIT, Bombay* (2000).

[18] K.A. MOHAMED, A.A. KHEDR, M.L. MISHREKY and A.A. ABDUL AZIM, *Surf. Tech*. 1982, 17, 11.

[19] G. BALACHANDRAN, M. L. BHATIA, N. B. BALLAL and P. KRISHNA RAO *ISIJ Int*. 2000, 40, (5) 491.

[20] "Standard practices for detecting susceptibility to intergranular attack in austenitic stainless steels" A262A, *Annual Book of ASTM standards*. (American Society for Testing of Materials, 2002).

[21] "Standard reference test method for making potentiostatic and potentiodynamic anodic polarization measurements" G5-94 *Annual Book of ASTM standards*. (American Society for Testing of Materials, 2004).

[22] Metals Hand Book, "Corrosion" 9th edition Vol. 13, (ASM International Pub. 1987), p. 320.

[23] "Standard Test Method for Pitting and Crevice corrosion resistance of stainless steels and related alloys by use of Ferric chloride solution." G48 *Annual Book of ASTM standards*. (American Society for Testing of Materials, 2000).

[24] P.J. UGGOWITZER, W.F. BAHRE, H. WOHLFROMM, and M.O. SPEIDEL, *Mater. Sci. Forum*. 1999, 318-320, 663.